Improved Maximum Entropy Method for Analysis of Fluorescence Spectroscopy Data: evaluating zero-time shift and assessing its effect on determination of fluorescence lifetimes

Journal:	*Analyst*
Manuscript ID	AN-ART-09-2015-001811.R1
Article Type:	Paper
Date Submitted by the Author:	22-Oct-2015
Complete List of Authors:	Esposito, Rosario; Università di Napoli Federico II, Dept. of Chemical, Materials and Production Engineering Mensitieri, Giuseppe; University of Naples Federico II, Dept. of Chemical, Materials and Production Engineering De Nicola, Sergio; CNR-SPIN,

SCHOLARONE™
Manuscripts

Improved Maximum Entropy Method for Analysis of Fluorescence Spectroscopy Data: evaluating zero-time shift and assessing its effect on determination of fluorescence lifetimes

Rosario Esposito[1,]*, Giuseppe Mensitieri[1] and Sergio de Nicola[2]

[1] Dept. of Chemical, Materials and Production Engineering, University of Naples Federico II, P.le Tecchio 80, 80125 Naples, ITA

[2] CNR-SPIN Napoli, Complesso Universitario di Monte Sant'Angelo, via Cinthia, 80126 Napoli, Italy

ABSTRACT

A new algorithm based on the Maximum Entropy Method (MEM) is proposed for recovering both the lifetime distribution and zero-time shift from time-resolved fluorescence decays intensities. The developed algorithm allows analysing complex time decays through an iterative scheme based on entropy maximization and Brent's method to determine the minimum of the reduced chi-squared value as a function of the zero-time shift.

The accuracy of this algorithm has been assessed through comparisons with simulated fluorescence decays both of multi-exponential and broad lifetime distributions for different values of the zero-time shift. The method is capable of recovering the zero-time shift with an accuracy better than 0.2% over a time range of 2000 ps. The center and the width of the lifetime distributions are retrieved with relative discrepancies that are lower than 0.1% and 1% for the multi-exponential and continuous lifetime distributions, respectively.

The MEM algorithm is experimentally validated by applying the method to fluorescence measurements of the time decays of the flavin adenine dinucleotide (FAD)

Introduction

The Maximum Entropy Method (MEM) is a powerful optimization mathematical algorithm widely applied in very diverse disciplines as image analysis, radio astronomy, medical imaging, pulse fluorimetry and fluorescence spectroscopy, to mention a few. The MEM avoids using a predetermined functional form, so it does not introduce artificial physics through a parametric fit and the basic way it accomplishes its task is by using a "regularizing function" as, for example, the well-known Shannon entropy which is maximized subject to the goodness of fit parameter constraint $\chi^2 \cong 1$[1–8].

It is of particular interest, in the present context, the possibility of applying the MEM approach in conjunction with several fluorescence spectroscopy techniques. Some relevant examples are briefly reported in the following.

In fact, the MEM algorithm is applicable in time-resolved single molecule fluorescence spectroscopy (SMFS). A relevant example of use of this technique is the probing at the molecular level, in a broad range of timescales, of the dynamics of polymer systems and their heterogeneity based on the stochastic occurrence of photoinduced effects and on proper procedures allowing the localization of single emission events with nanometer resolution. This high spatial resolution is attained by relying upon confocal technique by which, with adequate photostability of the investigated system, it is possible to collect dynamic data on single molecules for extended periods with high time resolution. Fluorescence intensities of single molecules as a function of time as well as fluorescence lifetimes of single molecules, with a resolution well below nanoseconds, can be measured[9–13]. To this regard, SMFS has been applied to the study of polymer dynamics and relaxation, since evaluation of local density fluctuations of a single dye molecule, based on the determination of fluorescence lifetimes and their distribution, allow gathering information on the presence of holes within the polymer matrix. The possibility of determining spatial and temporal heterogeneities in polymer systems can be exploited to visualize, in real time, the effects of changes in the environment on the structure of polymers, polymer networks, and polymer gels. Moreover, SMFS is useful also in the investigation of polymerization processes based on the evolution of molecular mobility during the reaction.

MEM methods are also useful in fluorescence correlation spectroscopy (FCS) which is a technique based on a correlation analysis of fluorescence signals that fluctuate as a consequence of the diffusion of molecules, thus allowing, under proper assumptions, to gather information on probe diffusivity[14]. Combination of FCS with confocal microscopy has been used to follow dynamics of individual polymer chains in several regimes (dilute, semidilute, reptation). The rotational and translational diffusion can be investigated in polymer solution, allowing also the study of processes like micellization and aggregation, the detection of heterogeneities on the nano to micrometer length scale, the diffusion of large nanoparticles in polymers and the diffusion of polymer chains at solid-liquid interfaces, to study of conformation of macromolecules in solvents and to study of crosslinking reactions[9–12]. In these cases, the analysis of molecular diffusion, complicated by the presence of different environments, can be performed by introducing diffusion time distributions that can be evaluated by solving the ill-posed problem of calculating the distribution of diffusion times from the autocorrelation function. This problem can be tackled by using MEM that provides a bias-free fitting of the data with a quasi-continuous distribution of a large number of diffusing components[15].

The dynamics of polymer chains is also investigated by using the so called fluorescence resonance energy transfer (FRET)[14]. For this purpose, at least one energy donor and one energy acceptor have to be present at well-defined positions in the polymer chain. The time resolved profile is described by a continuous lifetime distribution determined by the rate of energy transfer over distances typically in the ranges of *20-60 Å*. It turns out that a nonlinear least square fitting procedure does not provide always accurate information about FRET when analyzing complex fluorescence lifetime measurements. The MEM is a feasible alternative and, indeed, it has been successfully applied to determine the desired lifetime distribution without imposing any assumptions on the time-resolved decay data.

Recent advances in nanotechnology and nanomaterials have exploited new fluorescent probes designed by incorporating organic fluorophores in a polymer nanoparticle and have raised challenging problems in quantitative analysis of fluorescence lifetime distributions[16–18]. The basic effect is that the quantum yield of these probes increase dramatically, particularly for fluorophores with low quantum yield since one particle can contains several dyes molecules. The entrapment of these fluorophores has also the effect of enhancing the stability by reducing the photo bleaching. Quantum dot (QD) nanoparticles are fluorescent nanoparticles not coated with a

fluorescent dye because they are intrinsically fluorescent with attractive optical properties such as high photo stability and broad, tunable emission that can extend from the visible to the mid-IR, depending on the size and composition of the QD[19,20]. The possibility of incorporating QD in polymeric matrices is of particular interest for developing FRET based biosensors capable of monitoring target species in diverse environments[21–24]. QD have been introduced in polymer nanofibers[25] and it was found a significant broadening of the lifetime distributions for fiber with diameter below *500 nm*. Models containing a fixed number of prescribed exponential decay terms can fail to describe these broader distributions whereas MEM appears to be best suited in these cases[26].

The measured fluorescence intensity decay is commonly expressed as the convolution of the instrument response function (IRF) with an intensity decay model function. IRF is measured from the scattering of the excitation light pulse traveling the collection optical pathway and reaching the detector. Therefore, there is an unavoidable zero-time shift (ZTS) or delay with respect to the fluorescence emission decay. The ZTS is the major source of error in time resolved fluorescence analysis. It heavily affects the determination of the MEM distribution and the agreement between the model function and the measured fluorescence decays intensity that is usually described by the chi-squared value[4,27,28]. In general, it is very difficult to adjust ZTS and a reliable procedure within the framework of a MEM-based algorithm is still lacking. ZTS is often assumed as fitting parameter of multi exponential models but its correlations with other model parameters cannot guarantee its correctness when used for a MEM data analysis. For these reasons, a step-by-step procedure is usually employed for estimating the ZTS until a reduction in the final chi-squared is obtained. However, the efficacy of such a procedure always depends on the expertise of the operator and thus it is of the utmost importance to develop an algorithm capable of providing simultaneous lifetime distribution and accurate estimate of ZTS.

In this paper, we propose a new MEM algorithm for recovering both lifetime distribution in fluorescence decay and ZTS between instrument response function and fluorescence intensity decay function. The new method extends our previous work of Ref. [29] in two ways. First, it modifies the MEM algorithm by including ZTS correction and, second, it improves the convergence of the algorithm by handling the singularity behaviour close to the convergence of the iterative scheme of the previous approach.

The method is based on maximizing the Shannon entropy subject to the chi-squared constraint

$\chi^2 \cong 1$ through a procedure based on the Brent's Method[30] to determine the minimum of the reduced chi-squared value as a function of ZTS. Contrarily *to our* previous method*, the maximization procedure in this new* approach leads to an iterative scheme based on a system of linear equations which is written explicitly in terms of the vector of relative corrections.

In Sec. (1) we present the general formulation of the algorithm for recovering lifetime profiles without a priori knowledge of the zero-time shift. We show that the maximization of the Shannon entropy leads to a set of nonlinear equations which depends on the parameters governing the IRF. In Sec. (2), we investigate on how a numerical inaccuracy in the estimate of ZTS affects the determination of MEM lifetime distributions and we show that accurate estimate of ZTS is obtained by determining the minimum of the reduced chi-squared value regarded as a function of the ZTS.

The accuracy and efficacy of this approach has been tested by considering simulations both for the case of multi exponential decay and uniform lifetimes distributions with different values of the ZTS to be retrieved (Sec. (3)). We show that this approach is capable of recovering the ZTS with an accuracy of about 0.2% for both the cases**.** The largest relative errors for the multi exponential decay curves are exhibited by the fastest decay component whose value is comparable with the resolution limit of the experimental setup. In this case, the relative discrepancies range from *6%* to *2%* for the relative fluorescent amplitudes and from *13%* to *4%* for the lifetimes when increasing values of the ZTS are considered. The fluorescent parameters of the Gaussian lifetimes distributions are retrieved within one standard deviation and high accuracy. The center and the width of the lifetimes distributions are retrieved with relative discrepancies that are lower than 0.1% and 1% respectively for any given value of the ZTS. Finally in Sec. (4), the proposed algorithm has been experimentally validated by applying the method to fluorescence measurements of the time decays of the flavin Adenine Dinucleotide (FAD), a molecule that participates in many oxidation-reduction reactions of biological systems. The results have been compared with those reported in the recent literature.

1.   DESCRIPTION OF THE METHOD

The temporal behavior of the fluorescence intensity is usually modeled[31] as a discrete sum of exponential decays:

$$I(t,t_0) = \sum_{k=1}^{N} \alpha_k e^{-\frac{t-t_0}{\tau_k}} \qquad (1.1)$$

The lifetime τ_k is weighted by the amplitude factor α_k and ranges from the resolution limit τ_1 to the maximum decay time τ_N characteristic of the fluorophore under investigation. The time t_0 is explicitly included in eq. (1.1) to account for the ZTS between the fluorescence decay and the instrument response function $R(t)$ and lies on the raising region of the decay curve. We consider a Gaussian IRF:

$$R(t) = Ae^{-\frac{t^2}{w^2}} \qquad (1.2)$$

where A is an amplitude factor and the full width at half maximum (FWHM) is given by $1.665\ w$. The theoretical model for the comparison with experimental data $\{E_m\}$ is carried out by considering the convolution product of the intensity decay function $I(t,t_0)$ by the instrument response function $R(t)$:

$$T(t,t_0) = \int_{t_0}^{\infty} R(t-t')I(t',t_0)dt' \qquad (1.3)$$

Taking into account eqs. (1.1) and (1.2) and performing the Gaussian integrals, it can be shown that the convolution function $T(t,t_0)$ can be written in the following form:

$$T(t,t_0) = \sum_{k=1}^{N} C_k(t,t_0)\alpha_k$$

$$C_k(t,t_0) = \frac{\sqrt{\pi}wA}{2}\exp\left(\frac{t_0-t}{\tau_k} + \frac{w^2}{4\tau_k^2}\right)Erfc\left(\frac{t_0-t}{w} + \frac{w}{2\tau_k}\right) \qquad (1.4)$$

Eq. (1.4) shows that the convolution function can be written as a linear combination of the coefficients $C_k(t,t_0)$ weighted by the amplitude factors α_k. The coefficients $C_k(t,t_0)$ depend both on the characteristic parameters of the IRF, i.e., the amplitude A and the width w, and on the intensity decay data through the zero-time shift t_0 and the lifetimes τ_k.

The MEM algorithm selects the lifetime distribution $\{\alpha_k\}_{t_0}$ according to the model (1.4) that maximizes the Shannon entropy function S,

$$S(\alpha_1,...,\alpha_N) = \sum_{k=1}^{N} \alpha_k\left(1-\log(\alpha_k)\right) \qquad (1.5)$$

subjected to the reduced chi-squared condition

$$\chi^2(t_0) = \frac{1}{M} \sum_{m=1}^{M} \frac{\left(E_m - T(t_m, t_0)\right)^2}{\sigma_m^2} \quad 1 \tag{1.6}$$

In eq. (1.6) E_m is the measurement taken with error σ_m at time t_m and M is the number of measurements. The reduced chi-squared condition describes the agreement between the curve fitted with MEM and the experimental data.

The method of Lagrange multiplier is adopted to find the MEM solution as the extremal of the Lagrange function

$$\Lambda(\alpha_1, ..., \alpha_N, \lambda) = -S(\alpha_1, ..., \alpha_N) + \lambda\left(\chi^2(t_0) - 1\right) \tag{1.7}$$

where λ is the Lagrange multiplier. By imposing the condition $\nabla \Lambda(\alpha_1, ..., \alpha_N, \lambda) = 0$ we get the following set of $N+1$ nonlinear equations:

$$(\nabla \Lambda)_{\alpha_i} = \log(\alpha_i) - \frac{2\lambda}{M} \sum_{m=1}^{M} \frac{\left(E_m - \sum_{j=1}^{N} C_j(t_m, t_0)\alpha_j\right)}{\sigma_m^2} C_i(t_m, t_0) = 0$$

$$(\nabla \Lambda)_{\lambda} = \frac{1}{M} \sum_{m=1}^{M} \frac{\left(E_m - \sum_{j=1}^{N} C_j(t_m, t_0)\alpha_j\right)^2}{\sigma_m^2} - 1 = 0 \tag{1.8}$$

where the subscript i ranges from 1 to N.

The solution of this set of equations is obtained by solving iteratively the following set of linear equations:

$$H \cdot \delta \mathbf{x} = -\mathbf{F} \tag{1.9}$$

where we have defined the vectors $\mathbf{x} = \left(\alpha_1, ..., \alpha_N, \lambda \right)$ and $\mathbf{F} = \nabla \Lambda$. The matrix H is the Hessian matrix of the Lagrange function Λ:

$$H_{i,j} = \frac{\delta_{i,j}}{x_j} + \frac{2\lambda}{M} \sum_{m=1}^{M} \frac{C_i(t_m, t_0) C_j(t_m, t_0)}{\sigma_m^2} \qquad\qquad i, j \leq N$$

$$H_{i,N+1} = -\frac{2}{M} \sum_{m=1}^{M} \frac{C_i(t_m, t_0)}{\sigma_m^2} \left[E_m - \sum_{k=1}^{N} C_k(t_m, t_0) x_k \right] \qquad i \leq N, j = N+1 \qquad (1.10)$$

$$H_{N+1,N+1} = 0 \qquad\qquad i, j = N+1$$

At each iteration step, the approximated solution $\mathbf{x}^{new} = \mathbf{x} + \delta\mathbf{x}$ shifts the components of the vector $\mathbf{F}$ closer to zero to minimize the norm $f = 1/2\,\mathbf{F} \cdot \mathbf{F}$. The first N components of the vector $\mathbf{x}$ accounts for the MEM lifetimes distribution characterized by the minimum number of peaks needed to describe the time dependent fluorescence signal. It turns out that many components of the vector $\mathbf{x}$ are close to zero when the iterative scheme (1.9) converges to the solution of (1.8). This, in turn, implies that the diagonal elements of the matrix H in (1.10) tend to infinity, thus leading to a singular behavior of the matrix close to the convergence and making critical the application of the MEM

The proposed algorithm is capable of handling the singular behavior close to convergence of the iterative scheme by a proper reformulation of matrix equation as it will be discussed below. The system (1.9) can be written as follows:

$$H \cdot I \cdot \delta\mathbf{x} = -\mathbf{F} \qquad\qquad (1.11)$$

where the identity matrix I can be written in the following factorized form:

$$I = \begin{pmatrix} x_1 & 0 & . & 0 \\ 0 & x_2 & . & . \\ . & 0 & . & . \\ 0 & . & . & x_{N+1} \end{pmatrix} \cdot \begin{pmatrix} \dfrac{1}{x_1} & 0 & . & 0 \\ 0 & \dfrac{1}{x_2} & . & . \\ 0 & 0 & . & . \\ 0 & 0 & & \dfrac{1}{x_{N+1}} \end{pmatrix} \qquad\qquad (1.12)$$

By taking into account (1.11) and (1.12) it is easy to see that (1.9) can rewritten in terms of a matrix system for the vector of the relative corrections $\delta\mathbf{x}^{rel} = (\delta x_1/x_1, ..., \delta x_N/x_N)$, namely

$$H^{eq} \cdot \delta\mathbf{x}^{rel} = -\mathbf{F} \tag{1.13}$$

where the transformed matrix H^{eq} is given by:

$$H_{i,j}^{eq} = \delta_{i,j} + \frac{2\lambda}{M} x_j \sum_{m=1}^{M} \frac{C_i(t_m, t_0) C_j(t_m, t_0)}{\sigma_m^2} \qquad i, j \leq N$$

$$H_{i,N+1}^{eq} = -\frac{2}{M} x_{N+1} \sum_{m=1}^{M} \frac{C_i(t_m, t_0)}{\sigma_m^2} \left[E_m - \sum_{k=1}^{N} C_k(t_m, t_0) x_k \right] \qquad i \leq N, j = N+1$$

$$H_{N+1,j}^{eq} = -\frac{2}{M} x_j \sum_{m=1}^{M} \frac{C_j(t_m, t_0)}{\sigma_m^2} \left[E_m - \sum_{k=1}^{N} C_k(t_m, t_0) x_k \right] \qquad i = N+1, j \leq N$$

$$H_{N+1,N+1}^{eq} = 0 \qquad i, j = N+1$$

(1.14)

The advantage of (1.13) formulation over the original system (1.9) is twofold: (i) the matrix H^{eq} is not singular in the limit of $\mathbf{x}$ tending to zero since the matrix elements in (1.14) are proportional to components of $\mathbf{x}$; (ii) the accuracy with which the MEM distribution, solution of the nonlinear system (1.8), is retrieved is that of the relative components $\delta\mathbf{x}^{rel}$ which are explicitly determined through the iterative linear scheme (1.13).

The package *linsolve* of MatLab is adopted to solve (1.13) by applying the *LU* decomposition algorithm[32]. Once the new relative correction vector $\delta\mathbf{x}^{rel}$ is found, the Newton step is given by $\delta\mathbf{s} = \left(x_1\delta x_1^{rel}, ..., x_{N+1}\delta x_{N+1}^{rel} \right)$ and the updated approximation of the solution is calculated by adding $\delta\mathbf{s}$ to the vector $\mathbf{x}$ known at the previous iteration step:

$$\mathbf{x}^{new} = \mathbf{x} + \delta\mathbf{s} \tag{1.15}$$

Only negative components of $\mathbf{x}^{new}$ need to be seek since only positive values are required for the lifetimes distribution. In this case, the positiveness is enforced by using only a fraction of the step δs. According to the Newton approximation, the step δs is a descendent direction for the

norm $f = 1/2\, \mathbf{F} \times \mathbf{F}$:

$$\nabla f \cdot \delta \mathbf{x}^{rel} = (\mathbf{F} \cdot H^{eq}) \cdot (H^{eq^{-1}} \cdot \mathbf{F}) = -\mathbf{F} \cdot \mathbf{F} < 0 \tag{1.16}$$

The quadratic convergence is ensured once we are close enough to the solution. Conversely, the step δs does not necessarily decrease the norm f and the minimization is achieved by backtracking on the Newton direction. The new point is chosen according to condition

$$\mathbf{x}^{new} = \mathbf{x} + \varepsilon \cdot \delta \mathbf{s} \tag{1.17}$$

where ε is a number in the range from 0 to 1 that minimize f in the direction of δs and its value is retrieved by the MatLab routine *fminbnd* through the Golden Section Search algorithm[30].

The iterative scheme (1.13)-(1.17) allows to retrieve the lifetimes distribution $\{\alpha_k\}_{t_0}$ which maximize the Shannon entropy $S_{max}(t_0)$ subjected to the condition $\chi^2(t_0) = 1$. The distribution $\{\alpha_k\}_{t_0}$ is dependent on the choice of t_0.

To retrieve the value of ZTS we proceed by minimizing the reduced chi-square $\chi^2(t_0)$. An algorithm based on the *Brent's Method*[30] has been developed to this purpose. The approach relies on the fact that the chi-squared $\chi^2(t_0)$ is a function of the zero-time shift t_0 which exhibits a minimum $\chi^2(t_{0\,min})$ in correspondence of a t_0 value, $t_{0\,min}$. Deviations from this minimum can be fitted to a good approximation by a quadratic time dependent law. The value of the zero-time shift $t_{0,min}$ can be recovered by the following iterative scheme:

$$t_{0,min} = t_0 - \frac{1}{2}\frac{(t_0 - t_a)^2\left[\chi^2(t_0) - \chi^2(t_b)\right] - (t_0 - t_b)^2\left[\chi^2(t_0) - \chi^2(t_a)\right]}{(t_0 - t_a)\left[\chi^2(t_0) - \chi^2(t_b)\right] - (t_0 - t_b)\left[\chi^2(t_0) - \chi^2(t_a)\right]} \tag{1.18}$$

where t_0 is the previous estimate of the zero-time shift and $\chi^2(t_0)$ is the corresponding value of chi-squared.

According to the Brent's method, the minimum is always bracketed with the triplet of *points* $t_a <$ $t_0 < t_b$ such that the chi-squared value $\chi^2(t_0)$ is less than both $\chi^2(t_a)$ and $\chi^2(t_b)$. A degenerate case arises when the three points are collinear since eq. (1.18) cannot be used. However, in this case, the *Golden Section Search* technique can be applied.

In the next section we will report several numerical results and we will show that the algorithm is capable of providing ZTS to a precision of about 10^{-3}.

2.   Inaccurate zero-time shift and lifetime distributions

To analyze the effects of zero-time shift on the retrieval of lifetime distributions by the MEM we consider the characteristic parameters governing the fluorescence decay signal in a typical time-correlated single photon counting (TCSPC) experiment. We perform a simulation with 4096 data points that span a time scale of *25 ns* and $5{\times}10^{4}$ counts in the maximum. The data points have been obtained by convolving a three exponential model function with zero-time shift t_0 = *100 ps* by a Gaussian instrument response function *R(t)* whose *FWHM* is *120 ps*.

The three decay times are τ_1 = *100 ps*, τ_2 = *1000 ps* and τ_3 = *4000 ps* and the same value for the relative amplitudes α_k = *0.333 (k=1, 2, 3)* has been considered according to the eq. (1.4). Poisson noise statistics that affects the typical TCSPC measurements was simulated by using the routine *poissrnd* of Matlab.

The fluorescence parameters are retrieved from the analysis of the MEM lifetime distribution by letting the zero-time shift t_0 deviate from its nominal value t_0 = *100 ps*.

Figure 1(a) shows the normalized MEM spectra obtained for three different zero-time shift errors, Δt_0 = *-10, 0, 20 ps,* by considering *N* = *500* lifetimes equally spaced in $\log \tau$ between τ_{min} = *20 ps* and τ_{max} = 10^{4} *ps*. As it can be seen, the distributions exhibit a peak for each decay component whose location is affected by the ZTS uncertainty with particular reference to the fast decay times. The lifetime and amplitude estimates $\langle \tau_k \rangle$ and $\langle \alpha_k \rangle$ of the k-th decay component are given by:

$$\langle \tau_k \rangle = \frac{\sum_{j=1}^{N_k} \alpha_j \tau_j \Delta_j}{\sum_{j=1}^{N_k} \alpha_j \Delta_j}, \langle \alpha_k \rangle = \frac{\sum_{j=1}^{N_k} \alpha_j \Delta_j}{\sum_{j=1}^{N} \alpha_j \Delta_j} \qquad (2.1)$$

where N_k is the number of lifetimes that comprise the k-th peak and Δ_j is the spacing in $\log \tau$.

Figure 1(b) shows that the relative error between the values of the retrieved lifetimes τ_k and the theoretical ones increases with increasing Δt_0. The accuracy decreases with decreasing lifetime and a relative error larger than *80%* is attained for the lifetime τ=*100 ps* when Δt_0 is *10 ps* which

corresponds to two time channels of the TCSPC. On the other hand, an accuracy better than 8% is obtained for decay times larger than *1000 ps* and *|Δt₀|<10 ps*. Therefore, larger lifetimes are less affected by an inaccurate value of ZTS.

Figure 1(c) shows that a similar behavior for the estimated values of the relative amplitudes.

An error of *10 ps* on the ZTS causes a relative error larger than 20% for the relative intensities α_k corresponding to the larger decay time and an accuracy worse than about 30% is obtained for the intensity of the lifetimes $\tau=100\ ps$.

Figure 1(d) displays the reduced chi-squared value χ^2 as a function of the ZTS error Δt_0 and shows clearly that χ^2 attains at its minimum at $\Delta t_0=0$. Therefore, the best value of the reduced chi-square as a function of the ZTS is obtained at $t_0=100\ ps$.

3.   Results and discussion

To validate the performance of the proposed MEM method with the chi-squared minimization approach, we have performed numerical simulations of fluorescence intensities taking into account the effect of the zero-time shift uncertainty. The simulated curves refer to three exponential
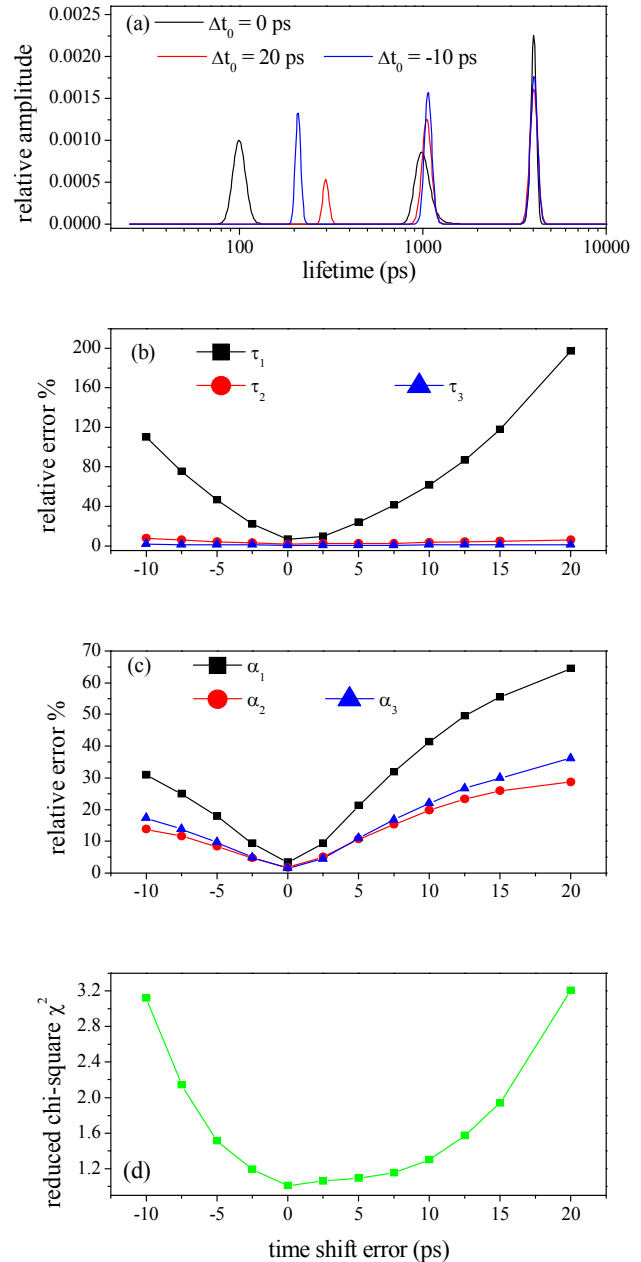
Figure 1. The effects of the errors Δt_0 in estimating the time shift t_0 on the MEM reconstruction. (a) The MEM lifetime distributions for different values of Δt_0. (b) The relative error in retrieving the lifetime decays as a function of time shift error. (c) The relative errors in retrieving the amplitude factors α_k. (d) The reduced chi-squared for different time shifts errors Δt_0. Results refer to a fluorescence decay intensities simulated by a three exponential function with lifetimes $\tau_1 = 100$ ps, $\tau_2 = 1000$ ps and $\tau_3 = 4000$ ps and the same value for the relative amplitude $\alpha_k = 0.333$ k = 1, 2, 3.

decays $\tau_1 = 100\ ps$, $\tau_2 = 1000\ ps$ and $\tau_3 = 4000\ ps$ with the same value for the relative amplitudes $\alpha_k = 0.333$ $(k=1,2,3)$ according to the Eq. (1.4) and span a time scale of $25\ ns$ with 5×10^4 counts in the maximum. Four different values of the zero-time shift, $t_0 = \pm500\ ps$ and $t_0 = \pm1000\ ps$, have been considered for investigating on the ability of the proposed method to retrieve the unknown temporal distance t_0 between the signal and the IRF together with the MEM lifetimes distribution.

It is well known that the main shortcoming of the MEM is retrieving the lifetimes distributions without estimation errors. To overcome this limitation and to investigate the performances of the proposed algorithm, a set of 20 synthetic curves has been generated for each zero-time shift value t_0. The fluorescence parameters and the zero-time shift are retrieved as average and standard deviation of the estimates calculated from the analysis of the MEM spectra for every set of curves. Figure 2(a) depicts the typical three exponential simulated curves generated for each value of the zero-time shift (closed circles) and the curves resulting from the fitting with the MEM algorithm (the solid colored lines) by considering $N = 500$ lifetimes equally spaced in $\log\tau$ between $\tau_{min} = 20\ ps$ and $\tau_{max} = 10^4\ ps$.

Figure 2(b) shows the typical normalized lifetimes distribution that is retrieved by the algorithm and accounts for the agreements between the simulated data and the fitted curves. The distribution exhibits a peak for each decay component. The mean position $\langle\tau_k\rangle$ and mean amplitude $\langle\alpha_k\rangle$ of the k-th peak are respectively the estimate of the lifetime and the pre-exponential factor of the k-th decay component as given by the eqs. *(2.1)*. The average and the standard deviation of the values $\langle\tau_k\rangle$, $\langle\alpha_k\rangle$ and t_0 resulting from each set of simulated curves are the estimates of the fluorescent parameters and have been reported in **Table 1**.

From the analysis of the numerical values, it results that the relative amplitudes α_k and the lifetimes τ_k are estimated by the MEM within one standard deviation and the estimated values are not affected by the zero-time shift value t_0. The relative errors exhibit the largest value for the fastest decay component and it can be ascribed to the fact that the decay time $\tau_1 = 100\ ps$ is comparable with the width of *120 ps* of the IRF, that is the lifetime is close to the resolution limit of the simulated experimental set up. Nevertheless, the relative discrepancies range from *6%* to *2%* for the relative amplitudes and from *13%* to *4%* for the lifetimes.
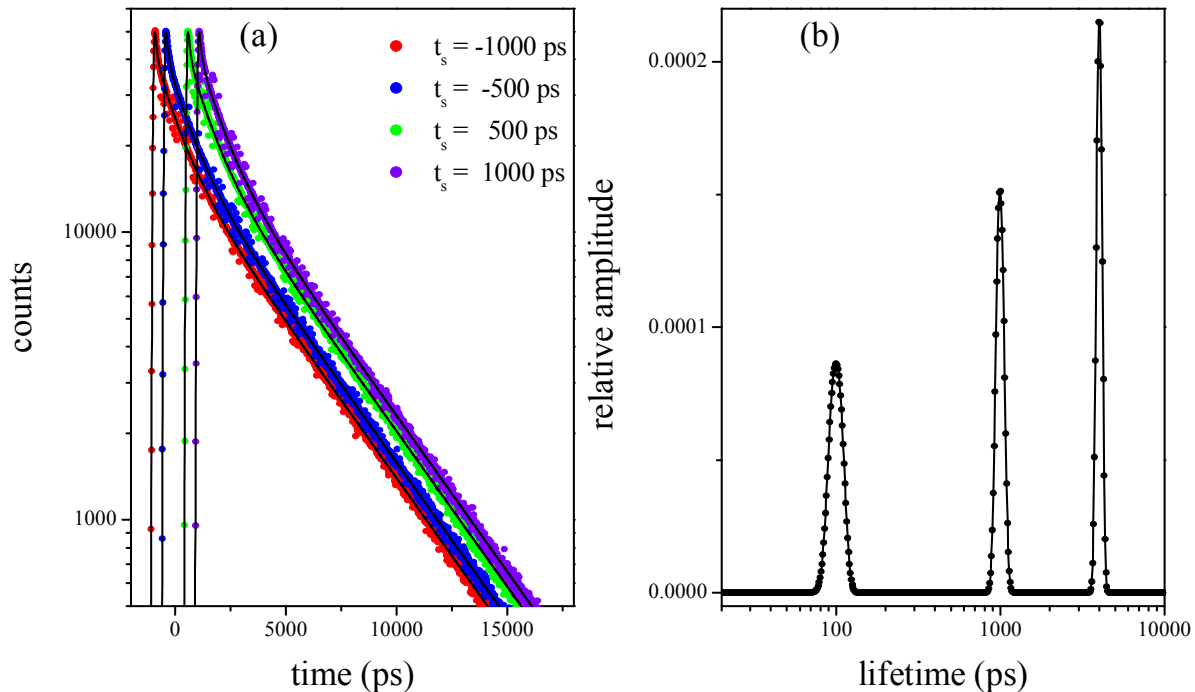
Figure 2. (a) The fluorescence decay intensities (colored closed circles) simulated by a three exponential function with lifetimes $\tau_1 = 100$ ps, $\tau_2 = 1000$ ps and $\tau_3 = 4000$ ps and the same value for the relative amplitude $\alpha_k = 0.333$. Four different values of the time shift t_0 have been considered, $t_0 = -1000$ ps (red circles), $t_0 = -500$ ps (blue circles), $t_0 = 500$ ps (green circles), $t_0 = 1000$ ps (violet circles). The solid black lines are the curves fitted with the MEM. (b) A typical normalized lifetimes distribution $\alpha(t)/\sum \alpha(t)\Delta$ that is obtained by the MEM analysis of a simulated noisy three exponential decay. The simulated data are comprised of *4096* data points on a time scale of *25 ns*. The MEM results are obtained for *N = 500* points equally spaced in *log* τ between *20 ps* and *10^4 ps* and are reported in Table 1

The agreement between estimated values and theoretical ones is impressive for the zero-time shift t_0 being the accuracy lower than *0.2%*, even though a range of values that spans *2000 ps* around the center of the IRF has been probed. The excellent accuracy in estimating the zero-time shift is the mainstay for the marked agreement between theoretical model function and experimental data as it has been evidenced in the previous section.

In order to test the performances of the proposed MEM algorithm in facing these cases, we have simulated fluorescent curves with a Gaussian lifetime distribution whose center is at $\tau_c = 3000$ *ps* and the standard deviation is *20%* of τ_c, that is $\Delta \tau = 600$ *ps*, and we have adopted the same analysis procedure of the multi exponential decays analysis. Thus, *20* curves have been simulated for each different values of the zero-time shift , $t_0 = \pm 500$ *ps* and $t_0 = \pm 1000$ *ps*, and each curve has been analyzed by running the MEM with *N = 500* lifetimes equally spaced in

14
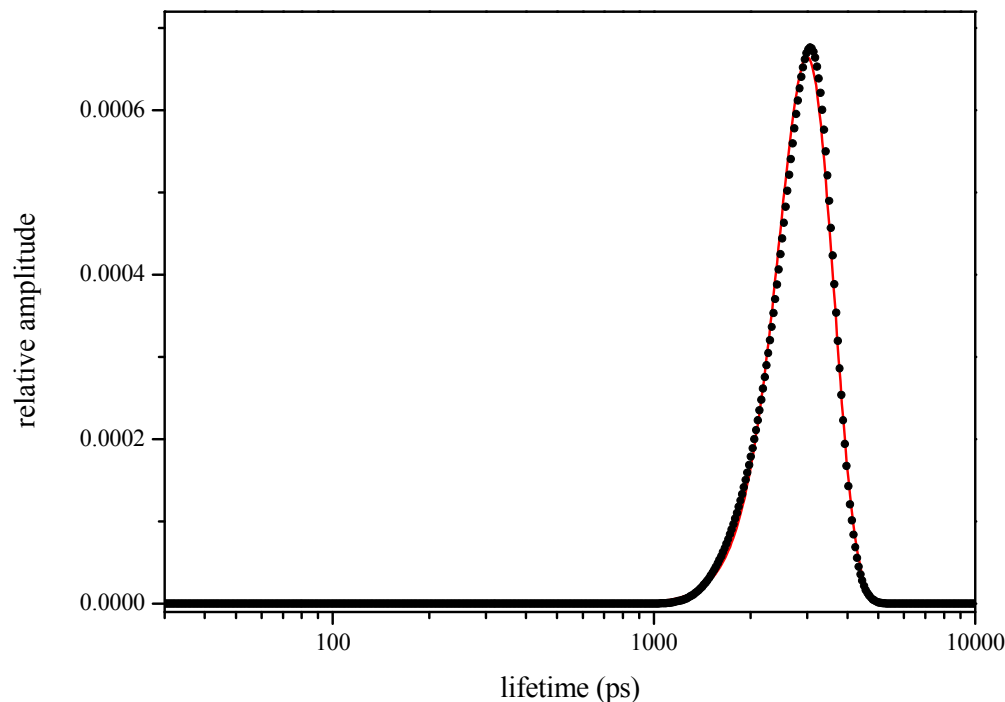
Figure 3. The black points are the normalized lifetime spectrum $\alpha(t)$ reconstructed by the MEM analysis performed on a fluorescence decay intensity with 5×10^4 counts in the peak channel for a Gaussian lifetimes distribution centered at $\tau = 3000\ ps$ with standard deviation $\Delta \tau = 600\ ps$. The MEM results are obtained for $N = 500$ points equally spaced in log τ between $20\ ps$ and $10^4\ ps$ and are reported in Table 1. The red solid line is the theoretical Gaussian lifetime distribution.

$\log \tau$ between $\tau_{min} = 20\,\text{ps}$ and $\tau_{max} = 10^4\,\text{ps}$. The black points profile of Figure 3 is the normalized MEM spectrum of any analyzed curve and the red solid line is the theoretical Gaussian lifetime distribution. The agreement between the retrieved spectrum and the theoretical one is excellent and the results of the statistical analysis on the retrieved fluorescent parameters have been reported in **Table 1**. The theoretical values have been predicted within one standard deviation and high accuracy as the case of the multi exponential decay. Particularly, the center and the width of the Gaussian lifetime distribution have been retrieved with relative discrepancies that are lower than 0.1% and 1% respectively for any value of the zero-time shift that is *re*covered with an accuracy better than 0.2%.

15

1
2
3
4
5
6
7
8
9
10
11
12
13
14
15
16
17
18
19
20
21
22
23
24
25
26
27
28
29
30
31
32
33
34
35
36
37
38
39
40

4.   Experimental test

Flavoprotein is a class of proteins that contain flavin as cofactor and participates in oxidation-reduction reactions in biological systems. In particular, Flavin Adenine Dinucleotide - FAD is a common member of the flavin family and it is present in various photoreceptors such as DNA-photolyase, phototropin, and 'blue-light using FAD' (BLUF) proteins[33–35]. Fluorescence investigations have shown that the isoalloxazine (ISO) ring is responsible for the light emission of FAD in the visible spectral range and is linked with adenine through hydrogen-bonding[36–39].

Recently, excited state fluorescence lifetimes measurements of FAD solutions at different pHs have been carried out with a time-correlated single-photon counting (TCSPC) set-up with a time resolution of *~40 ps*[36,40]. It has been reported that FAD decays at *pH = 7* exhibits a bi-exponential feature with two lifetimes of *4440 ps* and *2270 ps* having relative contributions of *36%* and *64%* respectively. The slow component represents the extended conformation of FAD in which the ISO and adenine rings interact through an unstacked conformation, as it has been confirmed by the estimated values of *4700 ps* for the decay time of flavin mononucleotide (FMN). Conversely, the fast component represents a partially stacked configuration in which the isoalloxazine moiety does not stack but interacts with the other parts of the molecule.

In order to test the efficacy of the MEM method with the chi-squared minimization approach

Table 1. The decay parameters and the time shift t_0 recovered by the MEM analysis

Multi exponential Decay							Gaussian distribution		
t_0 (ps)	α_1(%)	α_2(%)	α_3(%)	τ_1 (ps)	τ_2 (ps)	τ_3 (ps)	t_0 (ps)	τ_c (ps)	$\Delta\tau$ (ps)
-999.3±0.8	32±2	33.9±0.7	33.8±0.8	105±13	1010±80	4010±160	-999.4±0.8	3000±2	597±8
-499±1	32±2	34±1	34±1	107±13	1010±70	4010±150	-499.4±0.9	3001±2	599±7
501±1	32±2	33.9±0.9	33.7±0.9	104±12	1010±70	4010±150	501±1	3001±1	595±6
1000±1	33±1	33.6±0.6	33.6±0.7	104±13	1010±70	4010± 60	1001±1	3001±1	597±7

The multi exponential decay section reports the MEM analysis of a three exponential decay with lifetimes $\tau_1 = 100\ ps$, $\tau_2 = 1000\ ps$ and $\tau_3 = 4000\ ps$ and the same value for the relative amplitude $\alpha_k = 0.333$. The Gaussian distribution section shows the center τ_c and the width $\Delta\tau$ of the Gaussian lifetimes distributions recovered by the MEM. The nominal values of the Gaussian parameters are $\tau_c = 3000\ ps$ and $\Delta\tau = 600\ ps$. In each case, four different values of the time shift have been considered, $t_0 = \pm1000\ ps, \pm500\ ps$.

16

1
2
3
4
5
6
7
8
9
10
11
12
13
14
15
16
17
18
19
20
21
22
23
24
25
26
27
28
29
30
31
32
33
34
35
36
37
38
39
40
41
42
43
44
45
46
47
48
49
50
51
52
53
54
55
56
57
58
59
60

discussed in this contribution, we have applied the developed algorithm to analyze time resolved fluorescence experimental measurements of FAD at pH=7, performed with our experimental set-up, replicating the experiments reported by . Sengupta et al.[36]. The sample excitation was provided by a picosecond diode laser emitting pulses at a repetition rate of *10 MHz* and a wavelength of $\lambda = 405\ nm$. The laser beam was focused into a *10 mm* sample cell by a microscope objective lens. The fluorescence emission was detected at *90°* to the incident light beam to minimize the amount of transmitted or reflected beam light reaching the detector. A bandpass filter blocks the residual laser beam and allows only radiation with a wavelength of *520±10 nm* to reach the detector, the chosen wavelength range being close to the maximum of FAD fluorescence emission spectrum. The detection apparatus was composed of a fast multichannel plate photomultiplier tube and a TCSPC electronics. The instrument response function (IRF) determined by TCSPS was about *140 ps* FWHM. See Reference [41] for further details.
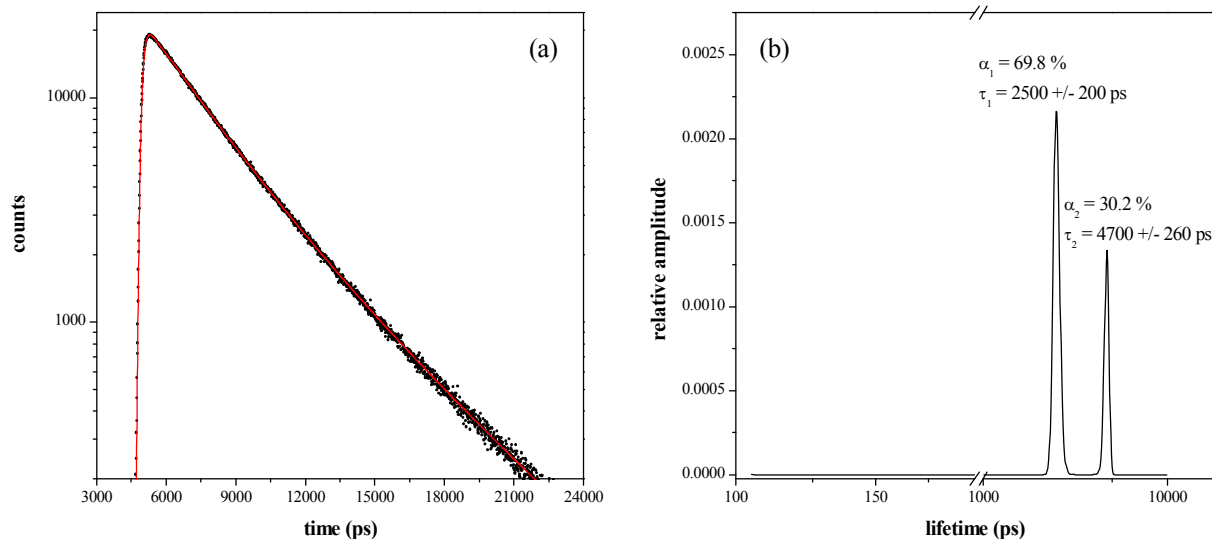
Figure 4. (a) Time resolved fluorescence signal of FAD at *pH=7* for an excitation wavelength *λ = 405 nm* (black points). The red solid line is the curve fitted with the MEM by considering *N = 500* points equally spaced in log τ between *10^2 ps* and *10^4 ps*. (b) Normalized lifetime spectrum reconstructed by the MEM analysis performed on a fluorescence decay intensity of FAD.
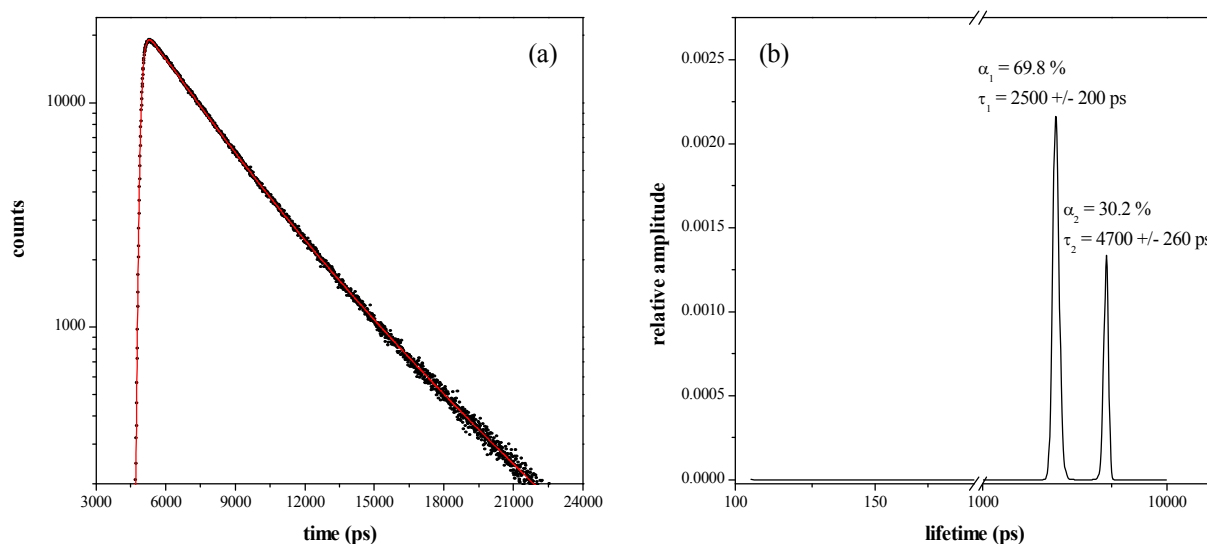
Figure 4(a) shows the experimental fluorescence decay curve of FAD at *pH = 7* (black points) and the curve fitted with the MEM algorithm by using *N = 500* points equally spaced in log τ between *10^2 ps* and *10^4 ps* (red solid line). The goodness of fit is ensured by a reduced chi-

18

squared value $\chi^2 = 1.18$. The normalized lifetimes distribution retrieved by the algorithm

(
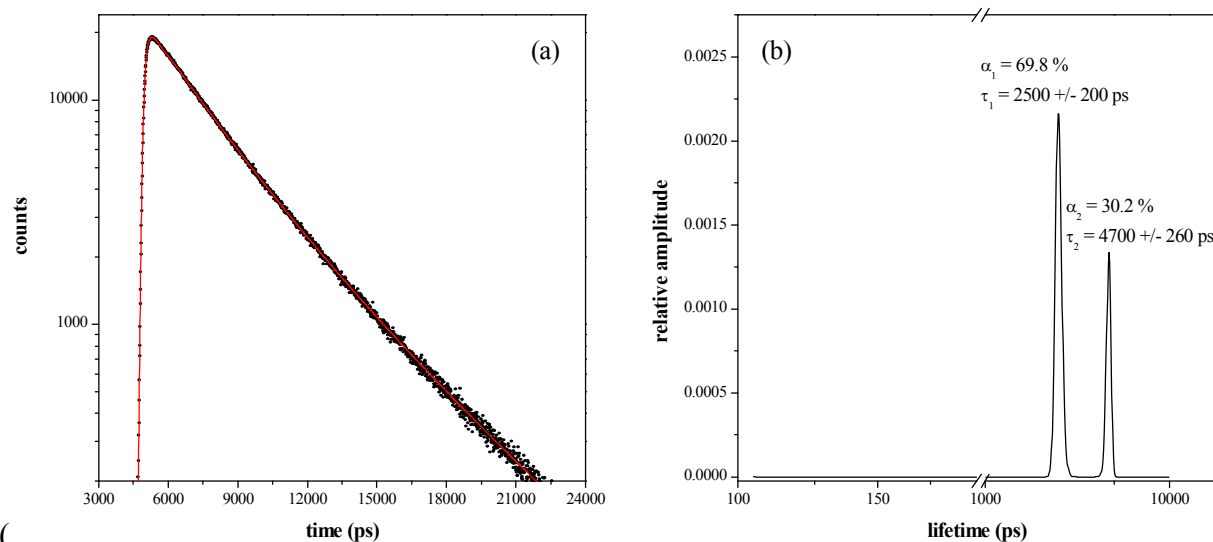
Figure 4(b)) exhibits two peaks corresponding to a fast and slow components. According to the equations (2.1), the estimated values of the fast and slow decay components are $\tau_1 = 2500 \pm 200$ ps and $\tau_2 = 4700 \pm 260$ ps with relative contributions of $\alpha_1 = 69.8\%$ and $\alpha_2 = 30.2\%$ respectively, in excellent agreement with the values reported and discussed extensively in Ref. [36].

Conclusions

The zero-time shift between the IRF function and the fluorescence decay epends in general on the collection optical pathway hat characterizes the experimental setup and the wavelength of the fluorescent signal. Fluorescence intensity decay exhibits both a multi exponential decay and a uniform lifetimes distribution.

Typical multi exponential models fail to describe the temporal behaviour of a fluorescent intensity when a complex decay is considered and/or an inaccurate estimate of the TZS is provided. MEM is a valid alternative to retrieve both multi exponential and continuum lifetimes distributions, but it is not prone to problems when estimate of the zero-time shift is inaccurate. Indeed, the relative error on time decays can be as high as *80%* even for ZTS error as low as *10 ps*.

The approach described here, based on MEM, allows to analyse complex time decays by retrieving both lifetime and zero-time shift through an iterative scheme based on entropy

maximization and Brent's Method. The accuracy of the proposed algorithm has been tested by considering both multi exponential and continuous lifetimes distributions for different values of the ZTS. The method is capable of providing ZTS to accuracy better than *0.2%* over a time range of 2000 ps.

Application of the method to multi exponential decay curves has shown that the largest relative errors are obtained by the fastest decay component whose value is comparable with the resolution limit of the experimental setup. Nevertheless, the discrepancies for the relative amplitudes range from *6%* to *2%* and for the lifetimes from *13%* to *4%*.

Numerical simulations have shown that the fluorescent parameters of the Gaussian lifetimes distribution can been retrieved within one standard deviation and high accuracy. The center and the width of the lifetimes distribution have been retrieved with relative discrepancies that are lower than 0.1% and 1% respectively. As regard as the influence of noise on the accuracy of the method we find that the accuracy does not depends significantly on the noise level when the number of counts exceeds $3\text{-}5\times10^{4}$. Indeed, we find results very similar to those reported in our previous work[29] (see, in particular, fig. 3 of Ref.[29])

The performance of the proposed MEM algorithm has also been tested experimentally by considering the fluorescence decay intensity of the FAD molecule in aqueous solution at pH = 7. The values of the time decay retrieved by the MEM spectrum are in agreement with those reported in the recent literature. Particularly, we notice the agreement between the estimated value of the slow decay component of FAD and the decay time measured for the FMN.

We point out that the assumption of a Gaussian IRF has allowed to express the maximization of the Shannon entropy in terms of a set et of nonlinear equations explicitly dependent on the parameters of the decay signal and on those of the IRF function. However, this assumption is not restrictive for the applicability of the method because the IRF function can always be deconvoluted in terms of a set of Gaussian functions.

REFERENCES

(1)   Gull, S. F.; Skilling, J. Maximum Entropy Method in Image Processing. *IEE Proc. F Commun. Radar Signal Process.* **1984**, *131*, 646.

(2)   Science, N.; Grant, F. Maximum Entropy Method of Data Analysis in Time-Resolved Spectroscopy. *Methods* **1994**, *240*, 262–311.

(3)   Maskevich, a. a.; Stsiapura, V. I.; Balinski, P. T. Analysis of Fluorescence Decay Kinetics of Thioflavin T by a Maximum Entropy Method. *J. Appl. Spectrosc.* **2010**, *77*, 194–201.

(4)   Livesey, A. K.; Brochon, J. C. Analyzing the Distribution of Decay Constants in Pulse-Fluorimetry Using the Maximum Entropy Method. *Biophys J* **1987**, *52*, 693–706.

(5)   Shaver, J. M.; McGown, L. B. Maximum Entropy Method for Frequency Domain Fluorescence Lifetime Analysis. 1. Effects of Frequency Range and Random Noise. *Anal. Chem.* **1996**, *68*, 9–17.

(6)   Steinbach, P. J.; Ionescu, R.; Matthews, C. R. Analysis of Kinetics Using a Hybrid Maximum-Entropy/nonlinear-Least-Squares Method: Application to Protein Folding. *Biophys. J.* **2002**, *82*, 2244–2255.

(7)   Esposito, R.; Altucci, C.; Velotta, R. Analysis of Simulated Fluorescence Intensities Decays by a New Maximum Entropy Method Algorithm. *J. Fluoresc.* **2013**, *6*, 234–239.

(8)   Brochon, J. C. Maximum Entropy Method of Data Analysis in Time-Resolved Spectroscopy. *Methods Enzymol.* **1994**, *240*, 262–311.

(9)   Xie, X. S.; Trautman, J. K. Optical Studies of Single Molecules at Room Temperature. *Annu. Rev. Phys. Chem.* **1998**, *49*, 441–480.

(10)   Deniz, A. A.; Laurence, T. A.; Beligere, G. S.; Dahan, M.; Martin, A. B.; Chemla, D. S.; Dawson, P. E.; Schultz, P. G.; Weiss, S. Single-Molecule Protein Folding: Diffusion Fluorescence Resonance Energy Transfer Studies of the Denaturation of Chymotrypsin Inhibitor 2. *Proc. Natl. Acad. Sci. U. S. A.* **2000**, *97*, 5179–5184.

(11)   Talaga, D. S.; Lau, W. L.; Roder, H.; Tang, J.; Jia, Y.; DeGrado, W. F.; Hochstrasser, R. M. Dynamics and Folding of Single Two-Stranded Coiled-Coil Peptides Studied by Fluorescent Energy Transfer Confocal Microscopy. *Proc. Natl. Acad. Sci. U. S. A.* **2000**, *97*, 13021–13026.

(12)   Zhuang, X.; Kim, H.; Pereira, M. J. B.; Babcock, H. P.; Walter, N. G.; Chu, S. Correlating Structural Dynamics and Function in Single Ribozyme Molecules. *Science* **2002**, *296*,

1473–1476.

(13)   Wöll, D.; Braeken, E.; Deres, A.; De Schryver, F. C.; Uji-i, H.; Hofkens, J. Polymers and Single Molecule Fluorescence Spectroscopy, What Can We Learn? *Chem. Soc. Rev.* **2009**, *38*, 313–328.

(14)   Wöll, D. Fluorescence Correlation Spectroscopy in Polymer Science. *RSC Adv.* **2014**, *4*, 2447.

(15)   Sengupta, P.; Garai, K.; Balaji, J.; Periasamy, N.; Maiti, S. Measuring Size Distribution in Highly Heterogeneous Systems with Fluorescence Correlation Spectroscopy. *Biophys. J.* **2003**, *84*, 1977–1984.

(16)   Zhang, J.; Lakowicz, J. R. Enhanced Luminescence of Phenyl-Phenanthridine Dye on Aggregated Small Silver Nanoparticles. *J. Phys. Chem. B* **2005**, *109*, 8701–8706.

(17)   Zhang, J.; Malicka, J.; Gryczynski, I.; Lakowicz, J. R. Surface-Enhanced Fluorescence of Fluorescein-Labeled Oligonucleotides Capped on Silver Nanoparticles. *J. Phys. Chem. B* **2005**, *109*, 7643–7648.

(18)   Novak, S.; Scarpantonio, L.; Novak, J.; Prè, M. D.; Martucci, A.; Musgraves, J. D.; McClenaghan, N. D.; Richardson, K. Incorporation of Luminescent CdSe/ZnS Core-Shell Quantum Dots and PbS Quantum Dots into Solution-Derived Chalcogenide Glass Films. *Opt. Mater. Express* **2013**, *3*, 729–738.

(19)   Bera, D.; Qian, L.; Tseng, T.-K.; Holloway, P. H. Quantum Dots and Their Multimodal Applications: A Review. *Materials (Basel).* **2010**, *3*, 2260–2345.

(20)   Pietryga, J. M.; Schaller, R. D.; Werder, D.; Stewart, M. H.; Klimov, V. I.; Hollingsworth, J. A. Pushing the Band Gap Envelope: Mid-Infrared Emitting Colloidal PbSe Quantum Dots. *J. Am. Chem. Soc.* **2004**, *126*, 11752–11753.

(21)   Kagan, C.; Murray, C.; Bawendi, M. Long-Range Resonance Transfer of Electronic Excitations in Close-Packed CdSe Quantum-Dot Solids. *Physical Review B,* 1996, *54*, 8633–8643.

(22)   Willard, D. M.; Carillo, L. L.; Jung, J.; Van Orden, A. CdSe-ZnS Quantum Dots as Resonance Energy Transfer Donors in a Model Protein-Protein Binding Assay. *Nano Lett.* **2001**, *1*, 469–474.

(23) Zammarano, M.; Maupin, P. H.; Sung, L. P.; Gilman, J. W.; McCarthy, E. D.; Kim, Y. S.; Fox, D. M. Revealing the Interface in Polymer Nanocomposites. *ACS Nano* **2011**, *5*, 3391–3399.

(24) Mérola, F.; Fredj, A.; Betolngar, D.-B.; Ziegler, C.; Erard, M.; Pasquier, H. Newly Engineered Cyan Fluorescent Proteins with Enhanced Performances for Live Cell FRET Imaging. *Biotechnol. J.* **2014**, *9*, 180–191.

(25) Meng, C.; Xiao, Y.; Wang, P.; Zhang, L.; Liu, Y.; Tong, L. Quantum-Dot-Doped Polymer Nanofibers for Optical Sensing. *Adv. Mater.* **2011**, *23*, 3770–3774.

(26) Virkki, K.; Demir, S.; Lemmetyinen, H.; Tkachenko, N. V. Photoinduced Electron Transfer in CdSe/ZnS Quantum Dot–Fullerene Hybrids. *J. Phys. Chem. C* **2015**, *119*, 17561–17572.

(27) Eaton, D. F. Recommended Methods for Fluorescence Decay Analysis. *Pure and Applied Chemistry*, 1990, *62*, 1631–1648.

(28) Van Den Zegel, M.; Boens, N.; Daems, D.; De Schryver, F. C. Possibilities and Limitations of the Time-Correlated Single Photon Counting Technique: A Comparative Study of Correction Methods for the Wavelength Dependence of the Instrument Response Function. *Chemical Physics*, 1986, *101*, 311–335.

(29) Esposito, R.; Altucci, C.; Velotta, R. Analysis of Simulated Fluorescence Intensities Decays by a New Maximum Entropy Method Algorithm. *J. Fluoresc.* **2013**, *23*, 203–211.

(30) Brent, R. P. *Algorithms for Minimization without Derivatives*; Englewood, N.; Cliffs, J., Eds.; Prentice-Hall series in automatic computation; Prentice-Hall, 1973.

(31) Lakowicz, J. R. *Principles of Fluorescence Spectroscopy*; 2nd ed.; Kluwer Academic/Plenum: New York.

(32) Golub, G. H.; Van Loan, C. F. *Matrix Computations*; Johns Hopkins Univ Pr, 1996; Vol. 3.

(33) Van Der Horst, M. A.; Hellingwerf, K. J. Photoreceptor Proteins, "Star Actors of Modern Times": A Review of the Functional Dynamics in the Structure of Representative Members of Six Different Photoreceptor Families. *Acc. Chem. Res.* **2004**, *37*, 13–20.

(34) Iseki, M.; Matsunaga, S.; Murakami, A.; Ohno, K.; Shiga, K.; Yoshida, K.; Sugai, M.; Takahashi, T.; Hori, T.; Watanabe, M. A Blue-Light-Activated Adenylyl Cyclase Mediates Photoavoidance in Euglena Gracilis. *Nature* **2002**, *415*, 1047–1051.

(35) Esposito, R.; Delfino, I.; Lepore, M. Time-Resolved Flavin Adenine Dinucleotide Fluorescence Study of the Interaction Between Immobilized Glucose Oxidase and Glucose. *Journal of Fluorescence*, 2013, 1–9.

(36) Sengupta, A.; Khade, R. V; Hazra, P. pH Dependent Dynamic Behavior of Flavin Mononucleotide (FMN) and Flavin Adenine Dinucleotide (FAD) in Femtosecond to Nanosecond Time Scale. *J. Photochem. Photobiol. A Chem.* **2011**, *221*, 105–112.

(37) van den Berg, P. A. W.; Feenstra, K. A.; Mark, A. E.; Berendsen, H. J. C.; Visser, A. Dynamic Conformations of Flavin Adenine Dinucleotide: Simulated Molecular Dynamics of the Flavin Cofactor Related to the Time-Resolved Fluorescence Characteristics. *J. Phys. Chem. B* **2002**, *106*, 8858–8869.

(38) Stanley, R. J.; MacFarlane, A. W. Ultrafast Excited State Dynamics of Oxidized Flavins: Direct Observations of Quenching by Purines. *J. Phys. Chem. A* **2000**, *104*, 6899–6906.

(39) Fujiwara, A.; Mizutani, Y. Photoinduced Electron Transfer in Glucose Oxidase: A Picosecond Time-Resolved Ultraviolet Resonance Raman Study. *J. Raman Spectrosc.* **2008**, *39*, 1600–1605.

(40) Sengupta, A.; Sasikala, W. D.; Mukherjee, A.; Hazra, P. Comparative Study of Flavins Binding with Human Serum Albumin: A Fluorometric, Thermodynamic, and Molecular Dynamics Approach. *Chemphyschem* **2012**, *13*, 2142–2153.

(41) Esposito, R.; Ventura, B. D.; De Nicola, S.; Altucci, C.; VELOTTA, R.; Mita, D. G.; LEPORE, M. Glucose Sensing by Time-Resolved Fluorescence of Sol-Gel Immobilized Glucose Oxidase. *Sensors* **2011**, *11*, 3483–3497.

1
2
3
4
5
6
7
8
9
10
11
12
13
14
15
16
17
18
19
20
21
22
23
24
25
26
27
28
29
30
31
32
33
34
35
36
37
38
39
40
41
42
43
44
45
46
47
48
49
50
51
52
53
54
55
56
57
58
59
60